DOI: 10.1002/chem.200601525

# Unique Ligand-Based Oxidative DNA Cleavage by Zinc(II) Complexes of Hpyramol and Hpyrimol

**Palanisamy Uma Maheswari,[a] Sharief Barends,[a] Seniz Özalp-Yaman,[a, e] Paul de Hoog,[a] Hélène Casellas,[a] Simon J. Teat,[b] Chiara Massera,[c] Martin Lutz,[d] Anthony L. Spek,[d] Gilles P. van Wezel,[a] Patrick Gamez,[a] and Jan Reedijk*[a]**

**Abstract:** The zinc(II) complexes reported here have been synthesised from the ligand 4-methyl-2-*N*-(2-pyridylmethyl)aminophenol (Hpyramol) with chloride or acetate counterions. All the five complexes have been structurally characterised, and the crystal structures reveal that the ligand Hpyramol gradually undergoes an oxidative dehydrogenation to form the ligand 4-methyl-2-*N*-(2-pyridylmethylene)aminophenol (Hpyrimol), upon coordination to $Zn^{II}$. All the five complexes cleave the $\phi$X174 phage DNA oxidatively and the complexes with fully dehydrogenated pyrimol ligands were found to be more efficient than the complexes with non-dehydrogenated Hpyramol ligands. The DNA cleavage is suggested to be ligand-based, whereas the pure ligands alone do not cleave DNA. The DNA cleavage is strongly suggested to be oxidative, possibly due to the involvement of a non-diffusible phenoxyl radical mechanism. The enzymatic religation experiments and DNA cleavage in the presence of different radical scavengers further support the oxidative DNA cleavage by the zinc(II) complexes.

**Keywords:** dehydrogenation · DNA cleavage · electrochemistry · oxidation · zinc

## Introduction

Research studies devoted to the design and synthesis of probes for elucidating the drug interaction sites on DNA and the so-called "chemical nucleases" have become increasingly important in the last thirty years.[1–3] The successful probes have wide applications as DNA sensors, antitumour drugs and artificial restriction enzymes, for example.[4,5] Among the different therapeutic strategies to eradicate cancer cells through DNA damage, the view of using small water-soluble transition-metal complexes, capable of oxidative or hydrolytic DNA cleavage as anti-cancer drugs, is a challenging topic in bioinorganic chemistry.[6,7] Many transition-metal complexes with V,[8] Fe,[9] Cu,[10,11] Co,[12] lanthanides,[13,14] and also actinides[15] have been reported as efficient DNA cleaving agents with or without sequence specificity. Of these metals, zinc is the second most abundant transition-metal ion present in the human body,[16,17] and is in the active sites of several enzymes such as superoxide dismutase, proteins containing zinc finger motifs and zinc hydrolases, in particular, owing to its Lewis acid character. Recently, much research has been aimed at preparing model zinc coordination complexes of these active sites for biomimetic purposes.[18] In this context, many zinc complexes

[a] Dr. P. U. Maheswari, Dr. S. Barends, Dr. S. Özalp-Yaman, P. de Hoog, Dr. H. Casellas, Dr. G. P. van Wezel, Dr. P. Gamez, Prof. J. Reedijk
Gorlaeus Laboratories, Leiden University
P.O. Box 9502, 2300 RA Leiden (The Netherlands)
Fax: (+31) 715-274-671
E-mail: reedijk@chem.leidenuniv.nl

[b] Dr. S. J. Teat
ALS, Berkeley Lab, 1 Cyclotron Road
MS2-400, Berkeley, CA 94720 (USA)

[c] Dr. C. Massera
Dipartimento di Chimica Generale ed Inorganica
Chimica Analitica, Chimica Fisica
Università degli Studi di Parma Parco Area delle Scienze
17A 43100 Parma (Italy)

[d] Dr. M. Lutz, Prof. A. L. Spek
Bijvoet Center for Biomolecular Research
Crystal and Structural Chemistry, Utrecht University
Padualaan 8, 3584 CH Utrecht (The Netherlands)

[e] Dr. S. Özalp-Yaman
Atilim University, Engineering Faculty
Chemistry Group, 06836 Ankara (Turkey)

Supporting information for this article is available on the WWW under http://www.chemeurj.org/ or from the author.

  

are known to be synthetic hydrolases towards the phosphodiester cleavage of the DNA macromolecule.[19–22]

Recently, we have reported the metal-assisted oxidation of the ligand 4-methyl-2-*N*-(2-pyridylmethyl)aminophenol (Hpyramol, which can be seen below along with its oxidised form, 4-methyl-2-*N*-(2-pyridylmethylene)aminophenol (Hpyrimol)) upon coordination to iron(II) or manganese(II).[23] This unusual feature has also been observed with copper(II) chloride, and a square-planar complex with the oxidised, dehydrogenated "pyrimol" is obtained.[24] Interestingly, this water-soluble copper complex cleaves DNA, oxidatively, without any reductant, suggesting a non-innocent participation of the ligand in the remarkable nuclease activity observed. The Hpyramol ligand is also dehydrogenated on coordination to the $Zn(acetate)_2$ salt and forms a trinuclear zinc complex as reported earlier by some of us.[25]

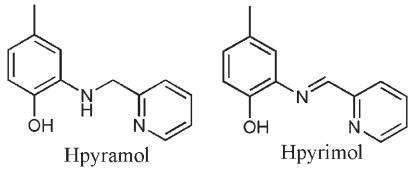


Because zinc is a biologically relevant metal ion,[26,27] the natural next step was to prepare various zinc(II) complexes with different anions, with the ligand Hpyramol, and to study the interaction of the resulting complexes with DNA. Accordingly, in the present paper, four new coordination complexes obtained by reaction of Hpyramol with zinc(II) chloride or zinc(II) acetate are described crystallographically. The cleaving abilities of all the zinc(II) complexes were examined by using $\phi$X174 phage DNA as a template, and the enzymatic religation experiments, together with the cell-transformation efficiencies, strongly suggest that the DNA cleavage is purely oxidative. The DNA-cleaving properties of these zinc complexes are rather surprising, as the zinc complexes are so far known to involve a hydrolytic pathway rather than an oxidative one. Thus, the DNA cleavage is suggested to be purely ligand-based, but the pure ligands themselves do not cleave DNA. Therefore, the zinc complexes reported here are the first zinc-based artificial nucleases performing oxidative DNA cleavage.

## Results and Discussion

**$Zn^{II}$–ligand complexes**: The ligand 4-methyl-2-*N*-(2-pyridylmethyl)aminophenol (Hpyramol) is obtained in a single-step reaction as previously described.[28] This ligand has been earlier reported as part of a trinuclear zinc(II) complex, namely, $[Zn_3(OAc)_4(pyrimol)_2]$ (**1**), in which it appeared to be oxidised to its planar pyrimol form.[25] Interestingly, this metal-assisted oxidation of Hpyramol is a very slow process, as evidenced by solution $^1H$ NMR studies.[25] By taking advantage of this slow reaction, the zinc complex bearing the original ligand, that is, Hpyramol, can be prepared by mixing concentrated solutions of the ligand and of the zinc(II) acetate in methanol, to increase the rate of the crystallisation process relative to the process that leads to the formation of pyrimol. In this manner, colourless crystals of $[Zn_2(OAc)_2(pyramol)_2]\cdot 2CH_3OH$ (**2**) have been isolated after two days, with a yield of 9% (based on the ligand). At this point, it should be mentioned that dark-red crystals of **1** are produced from the same mother liquor, but after two weeks, resulting in the dehydrogenated pyrimol ligand. The molecular structure of **2**, along with the atom labelling scheme, is illustrated in Figure 1. The dinuclear unit consists

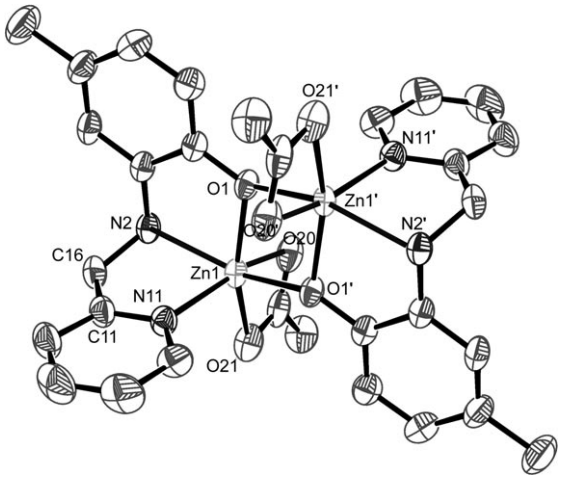


Figure 1. ORTEP perspective view of zinc(II) complex **2**. Hydrogen atoms and lattice solvent molecules have been omitted for clarity. Selected bond lengths [Å] and angles [°]: Zn1–O1 2.018(3), Zn1–O1′ 2.063(2), Zn1–O20 2.315(3), Zn1–O21 2.109(3), Zn1–N2 2.211(3), Zn1–N11 2.090(3); O1-Zn1-N11 104.93(11), N11-Zn1-O21 98.45(12), O21-Zn1-O20 58.40(11), O20-Zn1-O1 98.02(11), N2-Zn1-O1′ 156.73(11). Symmetry operation ′: $1-x, -y, 1-z$.

of two hexacoordinated Zn atoms bridged by the phenolate moieties of two deprotonated tridentate pyramol ligands, with an inversion centre located between the metal ions. The zinc atoms are in a highly distorted octahedral environment as a result of the bidentate coordination mode of the acetate anions. The equatorial plane is defined by the pyridine nitrogen atom N11 and the bridging phenolate oxygen atom O1 of a pyramol ligand and by the two oxygen atoms O20 and O21 from an acetato ligand (Figure 1). The in-plane angles range from 58.40(11) to 104.93(11)°, which reveals the distorted geometry. The equatorial Zn–N and Zn–O bond lengths[25,29] as well as the bond lengths observed for the bidentate acetate[30] can be considered as normal. The axial positions of the octahedron are occupied by the amine nitrogen atom N2 from a pyramol and the phenolate oxygen atom O1′ from a second pyramol ligand, at expected elongated bond lengths (Figure 1).[31]

The reaction of zinc(II) chloride with Hpyramol in acetonitrile gives rise to the formation of the crystalline complex $[Zn_2Cl_2(pyramol)_2]\cdot 2CH_3CN$ (**3**) within a day. Compound **3**

  

crystallises in the triclinic *P*1 space group. The ORTEP view of this dinuclear complex in which the zinc atoms are bridged by phenoxido moieties from two ligands is depicted in Figure 2. Each pentacoordinated zinc atom is in a distorted

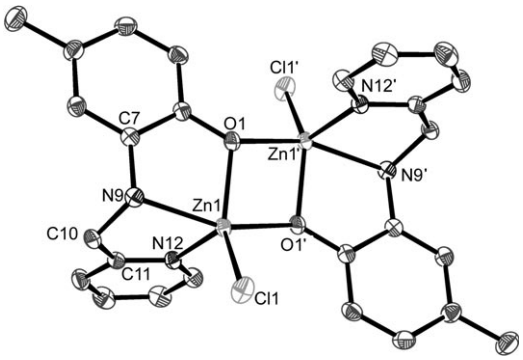


Figure 2. ORTEP perspective view of zinc(II) complex **3**. Hydrogen atoms and lattice solvent molecules have been omitted for clarity. Selected bond lengths [Å] and angles [°]: Zn1–O1 2.0192(10), Zn1–O1′ 2.0838(10), Zn1–Cl1 2.2575(4), Zn1–N9 2.2088(13), Zn1–N12 2.0658(12); O1-Zn1-Cl1 134.53(3), Cl1-Zn1-N12 116.22(4), N12-Zn1-O1 107.95(5), N9-Zn1-O1′ 155.39(5). Symmetry operation ′: 1−*x*, 1−*y*, 1−*z*.

trigonal-bipyramidal environment with a $\tau$ factor of 0.79 ($\tau=0$ for an ideal square-pyramidal geometry and $\tau=1$ for a perfect trigonal-bipyramidal environment).[32] The equatorial plane is defined by the pyridine N12 atom and the bridging phenolate O1 atom of a pyramol ligand, and by the chloride anion Cl1 (Figure 2).

The Zn–N, Zn–O and Zn–Cl bond lengths are in common ranges.[33,34] The in-plane angles vary from 107.95(5) to 134.53(3)°, which reflects the distortion induced by the ligand coordinating at equatorial–axial–equatorial positions, and by the bridging phenolato moieties that connect the two metal ions, separated by a short distance of 3.1772(2) Å. The axial positions of the trigonal bipyramid are occupied by the amine nitrogen atom N9 from the ligand and the phenolate O1′ atom from a second pyramol ligand at normal distances.[35] In addition, each dinuclear unit is interacting with two neighbouring complexes through π–π stacking between the pyridine rings, generating a one-dimensional (1D) supramolecular polymer (see Figure 3).

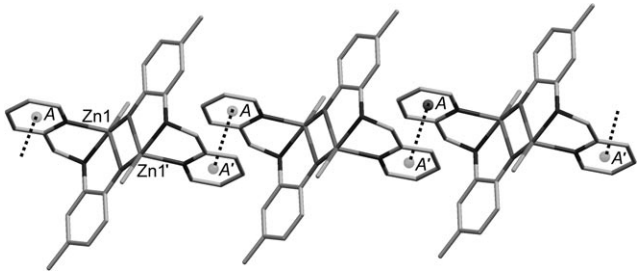


Figure 3. The π–π stacking interactions in complex **3** resulting in a 1D supramolecular polymer. Centroid *A*···centroid *A*′, 3.593 Å.

After one week, a new single crystal obtained from the same mother liquor (from which complex **3** had been isolated) was mounted on the diffractometer (see the Experimental Section for X-ray structure determination details) in order to investigate the metal-mediated oxidation of the amine function (Hpyramol) to the corresponding imine group (Hpyrimol). Interestingly, a significantly different solid-state structure was observed in this case (Figure 4).

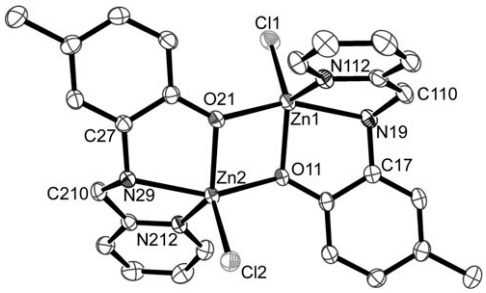


Figure 4. ORTEP perspective view of zinc(II) complex **4**. Hydrogen atoms have been omitted for clarity. Selected bond lengths [Å] and angles [°]: Zn1–O11 2.0031(14), Zn1–O21 2.0704(13), Zn1–Cl1 2.2587(6), Zn1–N19 2.2133(16), Zn1–N112 2.0788(17), Zn2–O21 2.0104(14), Zn2–O11 2.0716(13), Zn2–Cl2 2.2530(6), Zn2–N29 2.2167(17), Zn2–N212 2.0860(17); O11-Zn1-Cl1 122.41(5), Cl1-Zn1-N112 111.45(5), N112-Zn1-O11 125.24(7), N19-Zn1-O21 151.78(6), O21-Zn2-Cl2 125.43(4), Cl2-Zn2-N212 116.50(5), N212-Zn2-O21 117.51(6), N29-Zn2-O11 152.18(6).

The new complex, $[Zn_2Cl_2(pyramol)_2]$ (**4**), crystallises in the same space group, namely, *P*1. However, contrary to **3**, no lattice acetonitrile molecules are present for **4**, which results in a completely different crystal packing (see Figures 3 and 5). The dinuclear complex now consists of two distinct zinc

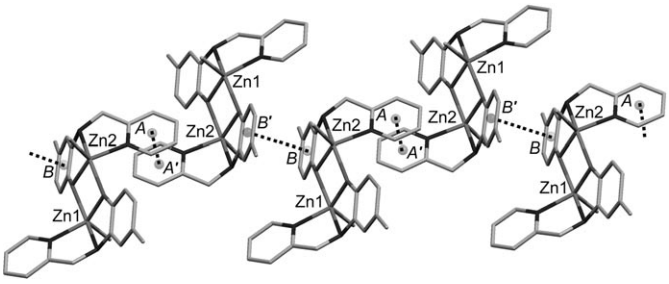


Figure 5. The π–π stacking interactions in complex **4** that result in a 1D supramolecular polymer. Centroid *A*···centroid *A*′, 3.828 Å; centroid *B*···centroid *B*′, 3.662 Å.

centres, Zn1 and Zn2, which exhibit slightly different coordination geometries. Zn1 is in a five-coordinate environment between the square pyramid and the trigonal bipyramid (with $\tau=0.44$).[32] Remarkably, the square-pyramidal character dominates for Zn1 ($\tau$ below 0.5), whereas both symmetry-related zinc atoms of **3**, for which the molecular formula of the dinuclear unit is identical to the one of **4**, are in a trigonal-bipyramidal environment. This geometry distortion, albeit less pronounced, is also observed for Zn2. Indeed, the

  

coordination geometry observed for Zn2 is also between the square pyramid and the trigonal bipyramid ($\tau = 0.58$),[32] but the trigonal-bipyramidal character is maintained ($\tau$ above 0.5). These important structural changes are apparently due to the pyramol ligands coordinated to Zn1 and Zn2, respectively. If the angle $\theta$ between the centroid of the pyridine ring, the nitrogen atom, and the centroid of the phenolate ring from a tridentate pyramol ligand coordinated to a zinc atom is considered (Figure 6), some drastic variations are clearly noticed (Table 1). This angle $\theta$ is 103° for both symmetrical metal centres of **3**, whereas the values are 136 and 114° for Zn1 and Zn2, respectively.

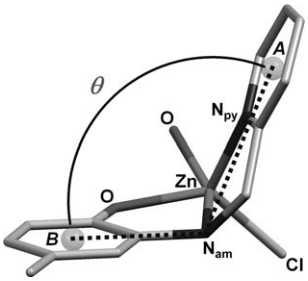


Figure 6. The $\theta$ angle between the pyridine centroid ($A$), the amine/imine nitrogen atom ($N_{am}$) and the phenol centroid ($B$) of the coordinated ligand.

Table 1. Observed $\theta$ angle(s) [°] for **3**–**5**.

| Complex | $A$-$N_{am}$-$B$ angle[a] [°] |
|---|---|
| **3** | 103.14(4) |
| **4** | 135.63(6) (Zn1), 114.18(6) (Zn2) |
| **5** | 172.47(5) |

[a] See Figure 6.

It thus appears that, for both ligands in **4**, this angle increases, indicating a propensity of the ligand pyramol to adjust its structural arrangement on the way to a more flat geometry; this suggests that the ligand is already adapting its conformation for a subsequent oxidation of the amine function to an imine, which will lead to the formation of the planar delocalised pyrimol moiety.[25] These steric variations result in a totally different crystal packing (Figure 5). Even more remarkable, π–π interactions also connect the dinuclear units to generate a 1D supramolecular polymer, but these π–π stacks now involve both the pyridine and the phenol rings (see Figure 5).

The fascinating oxidative transformation is confirmed by the X-ray diffraction analysis of red single crystals of $[Zn_2Cl_2(pyrimol)_2]$ (**5**), which are produced from the same reaction mixture after several weeks. It has to be pointed out here that this oxidised complex **5** can also be directly prepared within one week, by reaction of zinc(II) chloride and Hpyramol in acetonitrile in a sealed pressure tube at 105 °C (see the Experimental Section). Compound **5** crystallises in the monoclinic space group $P21/c$. The dinuclear moiety consists of two symmetry-related pentacoordinated zinc atoms (Figure 7). Their coordination environment is highly distorted, and lies between the trigonal-bipyramidal and square-pyramidal geometries ($\tau = 0.58$).[32] The Zn–N, Zn–O and Zn–Cl bond lengths can be considered as normal

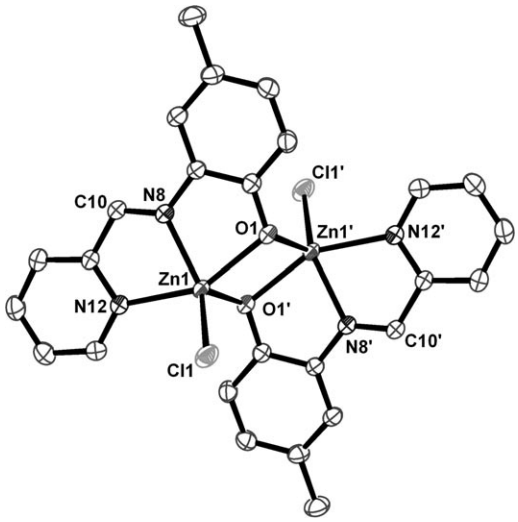


Figure 7. ORTEP perspective view of zinc(II) complex **5**. Hydrogen atoms have been omitted for clarity. Selected bond lengths [Å] and angles [°]: Zn1–O1′ 1.9894(10), Zn1–O1 2.1770(10), Zn1–Cl1 2.2269(4), Zn1–N8 2.0691(12), Zn1–N12 2.2113(13); O1′-Zn1-Cl1 111.00(3), Cl1-Zn1-N8 131.02(4), N8-Zn1-O1′ 117.55(5), N12-Zn1-O1 152.67(4). Symmetry operation ′: $-x, -y, -z$.

for this type of $N_2O_2Cl$ coordination set.[36,37] The equatorial plane is defined by the imine N8 atom and the bridging phenolate O1 atom of a pyramol ligand, and the chloride anion Cl1 (Figure 7). The in-plane angles range from 111.00(3) to 131.02(4)°, indicating a significant distortion of the trigonal-bipyramidal geometry. Contrary to **3** and **4**, the crystal packing of **5** does not show π–π interactions, which is most likely due to a completely different spatial arrangement of the planar molecules in the solid-state structure.

**DNA cleavage studies**: The DNA cleaving properties of the zinc(II)–pyramol/pyrimol complexes **1**–**5** prepared from zinc(II) chloride/acetate and Hpyramol have been investigated by using $\phi$X174 phage DNA. When $\phi$X174 DNA (20 μM in base pair (b.p.)) was incubated for eight hours with complexes **1**–**5** (100 μM) at 37 °C, in the absence of any reductant, the following order of cleavage efficiency, from supercoiled DNA (Form I) to nicked DNA (Form II) was observed (Figure 8): complex **5** (94 %) > complex **1** (75 %) > complex **4** (67 %) > complex **3** (57 %) > complex **2** (38 %). Thus, complexes **1** and **5**, bearing the (oxidised) pyrimol ligand, are significantly more active than complexes **2**, **3** and **4**. The free ligands Hpyramol and Hpyrimol have no cleavage activity. Accordingly, complexes **1** and **5** have been used to further investigate the nature of the DNA cleavage observed. Different concentrations of complex **5** (10–100 μM) were used to digest $\phi$X174 phage DNA (20 μM b.p.) at 37 °C for eight hours. A clear dependence of the DNA cleavage

  

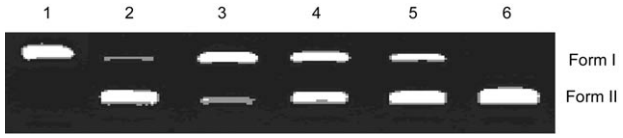


Figure 8. Agarose gel electrophoresis of $\phi$X174 phage DNA (20 μM b.p.) after 8 h incubation with zinc complexes **1**–**5** (100 μM), without reductant in phosphate buffer, pH 7.2, 37 °C. Lane 1, control; lane 2, complex **1**; lane 3, complex **2**; lane 4, complex **3**; lane 5, complex **4**; lane 6, complex **5**.

on the concentration of the zinc complex used was observed (Figure 9a). However, even at high concentrations of complex **5**, the linear form of DNA (Form III) was not detected, which is also the case for all the aforementioned zinc(II) complexes.

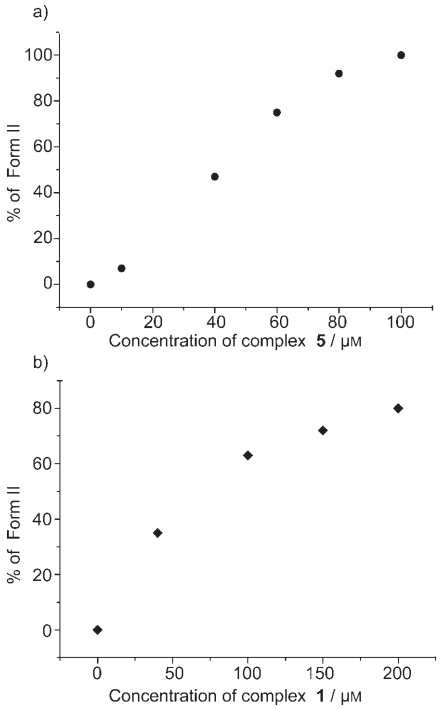


Figure 9. a) Plot of the different concentrations of complex **5** (used to digest $\phi$X174 phage DNA (20 μM)) versus the percentage of Form II formed after 8 h incubation at 37 °C. b) Plot of the different concentrations of complex **1** (used to digest $\phi$X174 phage DNA (20 μM)) versus the percentage of Form II formed after 8 h incubation at 37 °C.

When the digestion of DNA (20 μM b.p.) mediated by complex **5** (40 μM) was followed over time, only a stoichiometric conversion of Form I to Form II was observed (see Figure S1 in the Supporting Information). A similar non-catalytic DNA cleavage pattern was noticed for complex **1**, but with a lower efficacy relative to **5** (see Figure S2). Similar to **5**, **1** also shows a concentration dependent, stoichiometric cleavage of DNA (Figure 9b). As shown in Figures 9a and 9b, both the complexes **1** and **5** follow pseudo-first-order kinetics (single-exponential curves). The highest rate constant of 0.158 $h^{-1}$ was observed for complex **1** at a concentration of 200 μM, and a rate of 0.25 $h^{-1}$ was observed for complex **5** at a concentration of 100 μM, following pseudo-Michaelis–Menten conditions (Figures S3a and S3b in the Supporting Information).[38] True Michaelis–Menten conditions could not be applied, as the system is not catalytic, like the analogous Cu–pyrimol complex.[24]

The DNA cleavage reactions carried out with complexes **1** and **5** are not inhibited by the presence of various radical scavengers, that is, $NaN_3$, superoxide dismutase, DMSO, ethanol and $D_2O$. The use of distamycin, or an excess of NaCl also does not inhibit the cleavage of DNA, and Form II is still detected if the digestion is performed under argon, or by using dark conditions (Figure 10 and Figure S4 in the

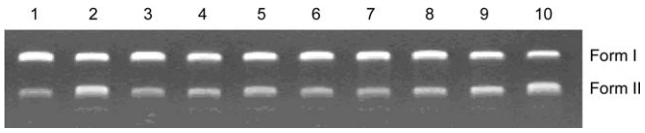


Figure 10. Agarose gel electrophoresis of the oxidative cleavage reaction of $\phi$X174 supercoiled phage DNA (20 μM b.p.) with the zinc complex **5** (40 μM) without reductant after an incubation time of 24 h at 37 °C in a phosphate buffer at pH 7.2 (lane 10), in the presence of the following: for lane 1, 200 μM $NaN_3$; for lane 2, 0.5 U of superoxide dismutase; for lane 3, DMSO; for lane 4, ethanol; for lane 5, 100 μM distamycin; for lane 6, $D_2O$; for lane 7, 350 μM NaCl; for lane 8, reaction performed under argon; for lane 9, reaction in the dark.

Supporting Information). These observations corroborate a hydrolytic pathway for the cleavage of DNA mediated by the zinc complexes.[3] Religation experiments on DNA cleavage products obtained from digestions with the zinc complexes **1**–**5** have been carried out to determine the nature of the DNA cleavage (Figure 11). Remarkably, these

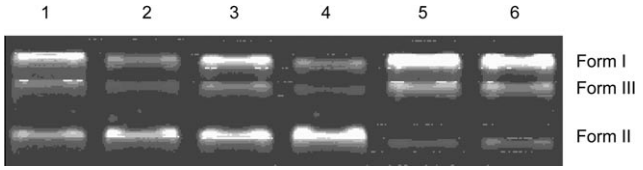


Figure 11. Agarose gel electrophoresis of the oxidative cleavage reaction. Lane 1: 20 μM DNA + complex **5**, 100 μM (blank); lane 2: DNA cleavage products from lane 1 treated with T4 ligase; lane 3: 20 μM DNA + complex **1**, 100 μM (blank); lane 4: DNA cleavage products from Lane 1 treated with T4 ligase; lane 5: 20 μM DNA + Hpyramol, 100 μM (blank); lane 6: DNA cleavage products from lane 5 treated with T4 ligase.

experiments clearly show that DNA cleavage mediated by zinc complexes **1**–**5** is not hydrolytic, but purely oxidative, because DNA cleavage products are not religated, whereas control $\phi$X174 DNA, digested by the restriction endonuclease PstI, is religated with a $>35\%$ efficiency (Figure S5 in the Supporting Information).

One can reasonably expect the involvement of radical species in the oxidative cleavage of DNA, which would be inhibited in the presence of radical scavengers during the digestion experiments. In the absence of evidence for any free

  

diffusible radical, a hydrolytic cleavage of the DNA strands may be anticipated. However, this mechanism is excluded because the nicked forms of the DNA digested by **5** or **1** are not religated by the T4 ligase enzyme. The results achieved from the experiments in the presence of various radical scavengers, and from the religation experiments show that a non-hydrolytic pathway not related to OH*, superoxide or singlet dioxygen is involved.[39]

To further investigate in detail the nature of the cleaving properties of **1** and **5**, pUC19 plasmid DNA treated with either complex **1** or **5** was relegated and was used for cell-transformation tests. As shown in Figure 12, the religation

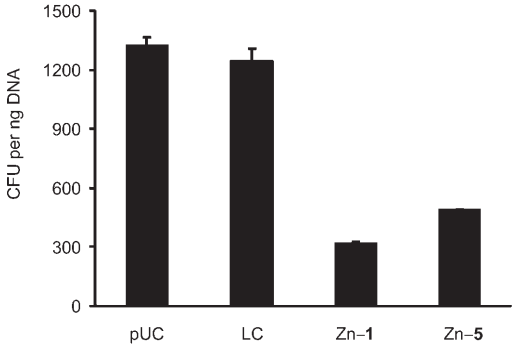


Figure 12. pUC19 plasmid DNA was treated with complex **5** or **1**, or linearised with endonuclease, PstI (New England Biolabs), and was subsequently purified for ligation as described in the Experimental Section. Competent *Escherichia coli* cells (strain JM109) were transformed with the ligation mixtures and plated on an ampicillin-containing medium. After 16 h of growth, colony-forming units were counted and expressed as CFU per ng of DNA. Untreated pUC19 plasmid DNA (pUC) was used for calculating the transformation efficiency (1325 ± 35 CFU per ng DNA). From ligation of the PstI-digested pUC19 (LC, 1242 ± 64 CFU per ng DNA), a ligation efficiency of ≈94% was calculated. Error bars denote the standard deviations of the means of three independent experiments.

of PstI-linearised pUC19 DNA (notated as LC) is achieved with an efficiency of about 94%. In contrast, the pUC19 DNA cleavage products, obtained from partial digestion with the zinc complexes **5** and **1**, do not show any cell transformations, because the observed colony-forming units are purely due to the presence of residual undigested supercoiled pUC19 DNA (Figure 12, and Figure S6 in the Supporting Information).

Traces of organic radical in complex **5** in the solid state have been detected by using EPR spectroscopy at room temperature. The amount of radical species present could not be determined, most likely due to their decaying or delocalised nature (Figure 13).[40] The radical is expected to originate from the phenolate moiety of the ligand coupled with the dehydrogenation of the Hpyramol ligand. Copper complexes with phenolate ligands are known in the literature as structural/functional models for the active site of the enzyme galactose oxidase.[41–43] This enzyme oxidises primary alcohols selectively to aldehydes by hydrogen abstraction in the presence of dioxygen, which is reduced to dihydrogen peroxide. The Cu–pyrimol complex also oxidises

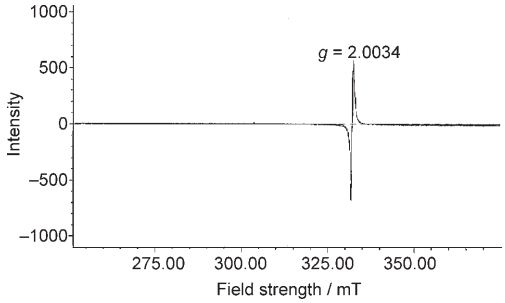


Figure 13. Solid-state powder EPR spectrum of complex **5**, recorded at room temperature.

benzyl alcohol selectively to benzaldehyde.[44] Accordingly, the catalytic DNA cleavage observed with the Cu–pyrimol complex can be explained by the initial hydrogen abstraction from the deoxyribose sugar in the presence of dioxygen, and generates dihydrogen peroxide in situ. Next, the dihydrogen peroxide couples with $Cu^{II}$ in a Fenton-type reaction to produce reactive oxygen species, which ultimately makes the DNA cleavage oxidative and catalytic. Similar results of oxidative DNA cleavage with Cu–salen type complexes, without any reductant, have been reported.[45] In the case of complexes **5** or **1**, the $Zn^{II}$ ions cannot play a redox role like $Cu^{II}$ and form hydrogen peroxide, so the DNA cleavage observed is strictly stoichiometric.

When the titration of complex **5** with calf-thymus DNA in a phosphate buffer at room temperature is followed by using UV-visible spectroscopy, the formation of phenoxyl radicals is evidenced after three hours of interaction. The intensity of the absorption bands initially observed for the complex **5** at $\lambda = 260$ and 305 nm increases upon addition of DNA at an $R$ value of 5 ($R = [DNA]/[metal\ complex]$, Figure 14). This hyperchromism is ascribed to the intercalation and π–π stacking interactions of the complex **5** between the DNA base pairs. The absorption band observed at 397 nm decreases and a new band around 420 nm appears. This band, which increases in intensity with time, is most

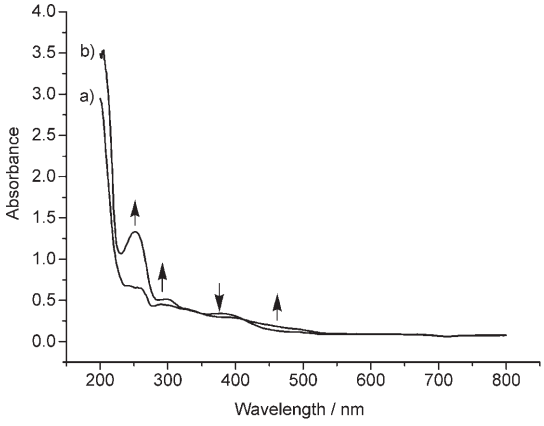


Figure 14. Absorption spectra of complex **5** in DMF diluted with 10 mM phosphate buffer at pH 7.2, in the absence (a; $R = 0$) and presence (b; $R = 5$) of calf-thymus DNA.

  

likely due to the formation of phenoxyl radical species, and is assigned to the π–π* transition of the phenoxyl radical, as MLCT bands are not occurring for zinc(II) systems.[46,47]

**Cyclic voltammetry studies**: Electrochemical investigations have been performed in order to appraise the role of the non-redox zinc(II) ions on the dehydrogenation of the ligand Hpyramol, and in the formation of the reactive phenoxyl radicals upon coordination. Therefore, the redox behaviour of the free ligands Hpyramol and Hpyrimol, and of the zinc complexes **1**–**3** and **5** have been investigated by using cyclic voltammetry at room temperature, under argon, in DMF with tetrabutylammonium hexafluorophosphate as the supporting electrolyte and with Ag/AgCl as the reference electrode. The electrochemical data are presented in Table 2. The cyclic voltammograms of the free ligand Hpyramol and its zinc(II) complexes **2** and **3** exhibit two-step oxidation processes. On reverse scan, a reversible cathodic peak is observed between −0.30 and −0.44 V, depending on the second oxidation peak (Figures 15, 16 and 17). On the other hand, the cyclic voltammogram of Hpyrimol and its zinc(II) complexes **1** and **5** show irreversible oxidation and reduction peaks as shown in Figures 15, 16 and 17. As the voltage scan rate increases, a linear dependence is observed, both between the peak current ($I_p$) and scan rate ($\nu^{1/2}$), and between the peak potential ($E_p$) and $I_p$, which suggests diffusion-controlled electron transfers.[48]

Table 2. Electrochemical data for the free ligands and the zinc complexes.

| Compound | $E_a$[a] [V] | $E_c$[b] [V] | $\Delta E_p$[c] [V] |
|---|---|---|---|
| Hpyramol | 0.71, 1.30 | −0.40[d,e] | 0.058 |
| Hpyrimol | 1.38 | −0.44[d,f] | 0.058 |
| complex **3** | 0.64, 1.25 | −0.30[d,e] | 0.058 |
| complex **5** | 1.32 | −0.36[d,f] | 0.056 |
| complex **2** | 0.51, 1.05 | −0.28,[e] −0.63[f] | |
| complex **1** | 0.84 | −0.22[f] | |

[a] Oxidation peak potential. [b] Reduction peak potential. [c] Difference between the peak potentials of the reversible cathodic peaks. [d] Reversible peak potential. [e] Dependant on the second oxidation peak potential. [f] Dependant on the first oxidation peak potential.

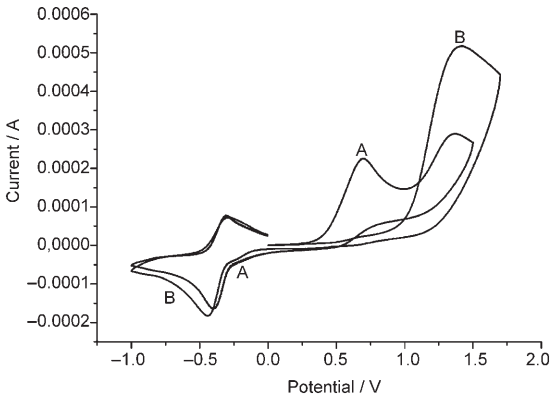


Figure 15. Cyclic voltammograms of 0.001 M Hpyramol (A) and 0.001 M Hpyrimol (B) in DMF, at room temperature, versus $Ag/Ag^+$.

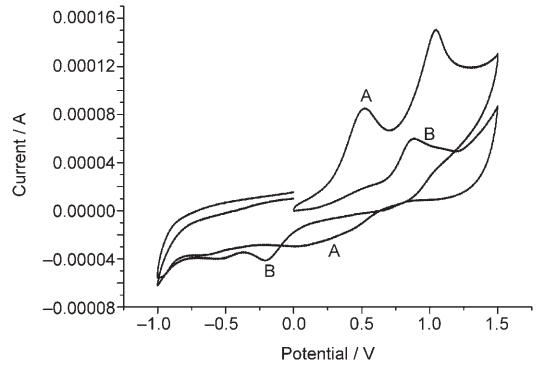


Figure 16. Cyclic voltammograms of 0.001 M complex **2** (A) and 0.001 M complex **1** (B) in DMF, at room temperature, versus $Ag/Ag^+$.

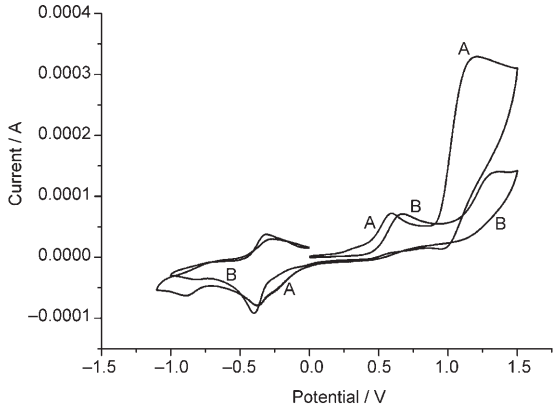


Figure 17. Cyclic voltammograms of 0.001 M complex **3** (A) and 0.001 M complex **5** (B) in DMF, at room temperature, versus $Ag/Ag^+$.

*Hpyramol*: The cyclic voltammogram (CV) of Hpyramol (Figure 15, Table 2) exhibits two irreversible oxidation peaks at around 0.71 and 1.30 V versus $Ag/Ag^+$, respectively. Upon reversal of the scan, a reversible oxidation peak at about −0.40 V versus $Ag/Ag^+$ appears and is dependent on the second oxidation peak (1.30 V). Two electrons were found to be transferred during the first oxidation peak of the ligand, based on chronocoulometry data, and are ascribed to the electrochemical dehydrogenation of the ligand. The number of electrons transferred during the second oxidation step could not be clearly established as it most likely involves the formation of phenoxyl radical species and further oxidative products. All these compounds appear to be very unstable and their formation is irreversible in the timescale of electrochemistry at room temperature.

*Hpyrimol*: The CV of the ligand Hpyrimol shows only one irreversible oxidation peak around 1.38 V versus $Ag/Ag^+$, and a reversible reduction peak around −0.44 V (Figure 15, Table 2). This observation is consistent with the results men-

  

tioned above for the ligand Hpyramol, and the oxidation peak is assigned to the formation of phenoxyl radical species that are very unstable and oxidised further to other oxidation products (quinone-type products, which are common for *para*-substituted phenols).[49]

*Complexes **1–3** and **5***: The two consecutive irreversible oxidation peaks observed with the Zn–pyramol complexes **2** and **3** (Table 2 and Figures 16 and 17) are assigned to the ligand dehydrogenation (pyramol to pyrimol), and to the phenoxyl radical formation and its consequent oxidation products, respectively (as observed for the free ligand Hpyramol). Similarly, the sole irreversible oxidation peak observed in the voltammograms of the Zn–pyrimol complexes **1** and **5** corresponds to the oxidation of the phenolic moiety to phenoxyl radicals, and the subsequent oxidation products. Thus, the coordination of the ligand to the zinc(II) ion clearly facilitates the oxidation of the ligand pyramol to pyrimol, because the amine/imine oxidation potential is observed around 0.51–0.67 V for the zinc complexes, whereas the value for this oxidation process is 0.71 V for the free ligand Hpyramol (see above). The above study indicates that the dehydrogenation of the ligand takes place for Hpyramol and its zinc complexes prior to the formation of the phenoxyl radical species. The phenoxyl radical species formed in the second oxidation step are very unstable and lead to other oxidation products. Controlled potential electrolysis for the free ligands and the zinc complexes has been performed at the second oxidation potentials. The electrolysed solutions are found to be EPR-silent both at room temperature and at low temperature (−15 °C), whereas the presence of radical species has been observed by means of powder EPR measurements on complex **5**. These disparate results can be explained by the great instability of the formed phenoxyl radical species in DMF (unfortunately, the zinc complexes are only soluble in DMF).

Thus, in the present study, it appears that the formation of highly reactive phenoxyl radical species in the presence of DNA is responsible for the observed oxidative cleavage of DNA by using the Zn–pyramol/pyrimol systems. The role of the zinc ions may be diverse: 1) The chloride or acetate anions of the zinc(II) salts may help to form the phenolate ions through deprotonation (however, it should be mentioned that the pure Hpyramol or Hpyrimol ligands that are not deprotonated do not cleave DNA); 2) The coordination of the ligand to the metal centre leads to perfect planar coordination compounds (complexes **1** and **5**), enabling them to intercalate and suitably interact with DNA for the cleavage process; 3) The coordination of the ligand Hpyramol to zinc favours its oxidation to pyrimol. From all the above observations, the degradation of the DNA through its interaction with the different zinc complexes appears to be a stoichiometric, oxidative cleavage event, most likely involving non-diffusible phenoxyl radical species originating from the ligand pyrimol. Detailed electro/spectroelectrochemical experiments are ongoing for a better understanding of the phenoxyl-radical-based mechanism.

## Conclusion

Reactions of $Zn(CH_3COO)_2$ and $ZnCl_2$ with the ligand Hpyramol yielded five different complexes (**1–5**), which were structurally characterised. The zinc(II) complexes **1** and **5** result from the slow dehydrogenation of the ligand in solution. Furthermore, the X-ray analyses have revealed an intermediate compound, **4**, which suggests that the slow oxidation of the ligand Hpyramol to anionic pyrimol occurs upon coordination to the $Zn^{II}$ ions. All five zinc complexes are able to oxidatively cleave DNA through the formation of putative radical-based active species, and the corresponding efficiencies are found to be in the following order (most efficient first): complex **5** (94 %) > complex **1** (75 %) > complex **4** (67 %) > complex **3** (57 %) > complex **2** (38 %). The complexes with the oxidised ligand are more active than those bearing the non-oxidised ligand. Traces of organic radicals have been observed in the solid-state EPR spectrum of complex **5**, which strongly suggests a non-diffusible radical mechanism for the herein reported oxidative cleavage of DNA.

## Experimental Section

**General**: All chemicals were used as obtained without further purification. Elemental analyses (C, H, N) were carried out by using a Perkin–Elmer 2400 series II analyzer. FTIR spectra were recorded by using a Perkin–Elmer Paragon 1000 FTIR spectrophotometer, equipped with a Golden Gate ATR device, by using the reflectance technique (4000–300 $cm^{-1}$). The ligand-field spectra of the compounds in solution were recorded in the $\lambda = 200$–1100 nm range with a Cary 50 spectrophotometer. $^1H$ NMR spectra were recorded by using a Bruker DPX 300 (300 MHz) instrument. Chemical shifts are reported in parts per million relative to the solvent peak. X-band EPR measurements were performed at 77 K in the solid state on a Jeol RE2x electron spin resonance spectrometer, by using DPPH ($g = 2.0036$) as the standard.

**4-Methyl-2-*N*-(2-pyridylmethylene)aminophenol (Hpyrimol)**: A solution of picolinaldehyde (10.7 g, 0.1 mol) in methanol (75 mL) was added, under constant stirring, to a solution of 2-amino-4-methylphenol (12.4 g, 0.1 mol) in methanol (50 mL) containing molecular sieves (4 Å). The reaction mixture was heated at reflux (70 °C) for 2 h. Next, the methanol was evaporated under reduced pressure to yield a deep-green residue. This solid material was redissolved in $CH_2Cl_2$ (200 mL), filtered and layered with *n*-hexane (200 mL). The resulting bilayer was left at −20 °C for the crystallisation of the pure compound. After two days, bright-yellow crystals were obtained. The crystals were collected and washed with diethyl ether, and were subsequently dried under argon. Yield: 53 %; $^1H$ NMR ($CDCl_3$): $\delta = 8.81$ (s), 8.72 (d), 8.20 (d), 7.82 (t), 7.37 (m), 7.25 (d), 7.2 (s), 7.1 (s), 7.06 (d), 6.90 (d), 2.31 ppm (s).

**$[Zn_2(OAc)_2(pyramol)_2]\cdot 2CH_3OH$ (2)**: A solution of Hpyramol (200 mg, 0.93 mmol) in methanol (20 mL) was added to a stirred solution of $Zn(CH_3COO)_2\cdot 2H_2O$ (280 mg, 1.28 mmol) in methanol (20 mL). The resulting reaction mixture was left unperturbed for the slow evaporation of the solvent. After a few days, colourless rectangular single crystals of **2**, suitable for X-ray diffraction analyses, were obtained. Yield (based on the ligand): 9 % (30.9 mg); IR (neat): $\tilde{\nu} = 3201$ (s, N–H), 1598, 1498, 1428, 1290, 807, 771, 674, 622, 485 $cm^{-1}$; elemental analysis calcd (%) for $C_{30}H_{32}N_4O_6Zn_2$ [**2**−2 $CH_3OH$]: C 53.35, H 4.78, N 8.30 %; found: C 52.44, H 4.30, N 8.36.

**$[Zn_2Cl_2(Pyramol)_2]\cdot 2CH_3CN$ (3)**: A warmed solution of $ZnCl_2$ (127 mg, 0.93 mmol) in acetonitrile (10 mL) was added to a stirred solution of Hpyramol (200 mg, 0.93 mmol) in acetonitrile (10 mL). The resulting re-

  

action mixture was stirred at 50 °C for 10 min and the solution was subsequently filtered. The filtrate was left unperturbed in air for the slow evaporation of the solvent. Yellowish-white crystals of **3**, suitable for X-ray diffraction analyses, were obtained after one day. Yield (based on the ligand): 37 % (109 mg); IR (neat): $\tilde{\nu}=3244$ (s, N−H), 1499, 1282, 1024, 807, 766, 488 $cm^{-1}$; elemental analysis calcd (%) for $C_{26}H_{26}N_4O_2Zn_2$ [**3**−2 $CH_3CN$]: C 49.71, H 4.17, N 8.92; found: C 49.19, H 3.63, N 9.07.

**$[Zn_2Cl_2(Pyramol)_2]$ (4)**: When the solution mentioned in the above procedure was left in air for about two weeks, the initially colourless crystals turned orange. These single crystals of **4** were analyzed by X-ray crystallography. Yield (based on the ligand): 34 % (99 mg); IR (neat): $\tilde{\nu}=3246$ (s, N−H), 1499, 1281, 1024, 808, 766, 488 $cm^{-1}$; elemental analysis calcd (%) for $C_{26}H_{26}Cl_2N_4O_2Zn_2$ (**4**): C 49.71, H 4.17, N 8.92; found: C 48.97, H 3.64, N 8.95.

**$[Zn_2Cl_2(Pyrimol)_2]$ (5)**: A solution of Hpyramol (500 mg, 2.32 mmole) in acetonitrile (15 mL) was added to a solution of $ZnCl_2$ (316 mg, 2.32 mmole) in acetonitrile (10 mL). The resulting reaction mixture was stirred for 10 min and was then placed in a sealed pressure tube, at 105 °C in an oven, for one week. At regular time intervals, the pressure tube was shaken to ensure the homogeneity of the solution. After a week, deep-red crystals of **5** were obtained and were analyzed by using X-ray crystallography. The same complex **5** could also be obtained by mixing equimolar amounts of the ligand Hpyramol and $ZnCl_2$ in warm acetonitrile. The reaction mixture was stirred at 50 °C for 1 h, filtered, and the filtrate was left unperturbed in air for the slow evaporation of the solvent for about two months. Yield (based on the ligand): 27 % (78 mg); IR (neat): $\tilde{\nu}=1608$ (s, N=C), 1506, 1281, 1255, 1219, 1020, 818, 774, 766, 644, 506, 414 $cm^{-1}$; elemental analysis calcd (%) for $C_{26}H_{22}Cl_2N_4O_2Zn_2$ (**5**): C 50.03, H 3.55, N 8.98 %; found: C 49.60, H 3.87, N 9.22.

**Procedure for DNA cleavage experiments**: $\phi$X174 DNA was purchased from Invitrogen, and was stored at −20 °C. The typical reaction mixture, containing double-stranded DNA and the zinc complexes **1**–**5** in a 10 mM phosphate buffer solution (pH 7.2), was incubated at 37 °C for the required time, with or without additives. After the incubation period, the reaction was quenched at −20 °C, followed by the addition of loading buffer (bromophenol blue, xylene cyanol, and 25 % ficoll). This reaction mixture was then loaded on a 0.8 % agarose gel containing ethidium bromide (2.54 μM final concentration in the gel as well as in the buffer). The gels were run at a constant voltage of 80 V for 60–90 min in tris–borate–EDTA (TBE) buffer containing ethidium bromide. After being washed with distilled water, the gels were visualised under a UV transilluminator and the bands were documented and quantified by using a BioRad Gel Doc 1000 apparatus interfaced with a computer.

**Enzymatic religation and cell-transformation experiments**: Double-stranded DNA was treated with the zinc complexes, without any reductant, at 37 °C and at pH 7.2. DNA samples were purified over QIAquick PCR purification columns (Qiagen) and were used for religation experiments. Control DNA was digested with the endonuclease PstI and cleaned in the same way. Ligation was performed in the 20 μL range by using 50 ng of the digested DNA products with 2 units of T4 DNA ligase (Fermentas) for 16 h at 16 °C. Competent JM109 cells were transformed in triplicate with the ligation mixtures and three different quantities were plated on ampicillin-containing medium. Religation of the PstI-linearised DNA revealed that ligation efficiency was around 94 %.

**Electrochemical studies**: The electrochemical behaviour of the free ligands and the complexes **1**–**3** and **5** was investigated by means of cyclic voltammetry (CV) in dimethylformamide (DMF) containing 0.1 M $(Bu_4N)PF_6$ as the supporting electrolyte. A three-electrode system containing a platinum-wire working electrode, a platinum-plate (counter) electrode and an Ag/AgCl reference electrode was used. The three electrodes were positioned as close as possible to minimise the Ohmic potential drop. Voltammetric recordings were performed under an argon atmosphere, at RT. The concentration of the free ligands and the complexes was 0.001 M for each measurement and the voltage scan rate during the CV measurements was 100 $mV\,s^{-1}$. Controlled potential electrolyses at the peak potentials were carried out in DMF versus Ag-wire reference electrode, taking into account the required correction between the $Ag/Ag^+$ and the Ag-wire systems (the oxidation potential of the ferrocene/ferrocenium couple was found to be 0.55 V vs. $Ag/Ag^+$ and 0.49 V vs. Ag wire in our system). Platinum-gauze electrodes were used as working and counter electrodes, respectively.

**X-ray crystallography**: X-ray intensities for complexes **2**–**4** were collected by using a Nonius–Kappa CCD diffractometer with rotating anode. The structures were solved by using direct methods (compound **2** with SHELXS-97,[50] compound **4** with SIR-97)[51] or automated Patterson methods (compound **3**, DIRDIF-99),[52] and refined with SHELXL-97[53] against $F^2$ of all reflections. Non-hydrogen atoms were refined freely with anisotropic displacement parameters. All hydrogen atoms were located in the difference Fourier map. The N−H and O−H hydrogen atoms were refined freely with isotropic displacement parameters; C−H hydrogen atoms were refined by using a riding model. In **2**, one methanol molecule was fully occupied, whereas the second molecule was only partially occupied. Geometry calculations and checking for higher symmetry were performed with the PLATON package.[54] The measurements for compound **5** were made by using Si(111) monochromated synchrotron radiation ($\theta=0.6894$ Å) and a Bruker APEX II CCD diffractometer by using standard procedures and programs for Station 9.8 of the Daresbury SRS (synchrotron radiation source).[55] Data were collected on a Bruker APEX II CCD diffractometer by using the APEX 2 software and processed by using SAINT Version 7.06a. The crystal was mounted onto the diffractometer at low temperature under nitrogen at approximately 150(2) K. The structure was solved by using direct methods with the SHELXTL program package. All non-hydrogen atoms were refined anisotropically. The function minimised was $[w(F_o^2-F_c^2)]$ with reflection weights $w-1=[2F_o^2+(g_1P)^2+(g_2P)]$, in which $P=[F_{o\,(max)}^2+2F_c^2]/3$. Table S1 in the Supporting Information includes the most relevant crystallographic parameters along with further details of the crystal structure determinations.

CCDC-609506 (**2**), -609507 (**3**), -609508 (**4**) and -609509 (**5**) contain the supplementary crystallographic data for this paper. These data can be obtained free of charge from The Cambridge Crystallographic Data Centre via www.ccdc.cam.ac.uk/data_request/cif.

## Acknowledgements

This work has been supported financially by the Graduate Research School Combination "Catalysis", a joint activity of the graduate research schools NIOK, HRSMC and PTN. Financial support from COST Action D21/003/01, Dutch WFMO (Werkgroep Fundamenteel-Materialen Onderzoek), CW (Foundation for the Chemical Sciences), NWO and EET are gratefully acknowledged. Professor Jaap Brouwer is thanked for support in performing the biological experiments. We acknowledge the provision of time with the Small Molecule Crystallography Service at the CCLRC Daresbury Laboratory through support by the European Community—Research Infrastructure Action under the FP6 "Structuring the European Research Area" Programme (through the Integrated Infrastructure Initiative "Integrating Activity on Synchrotron and Free Electron Laser Science"). Dr. Ronald Hage (Unilever Research, Vlaardingen, NL) is thanked for his comments and suggestions on the electrochemical studies.

[1] L. J. K. Boerner, J. M. Zaleski, *Curr. Opin. Chem. Biol.* **2005**, *9*, 135.
[2] J. A. Cowan, *Curr. Opin. Chem. Biol.* **2001**, *5*, 634.
[3] A. Nomura, Y. Sugiura, *Inorg. Chem.* **2004**, *43*, 1708.
[4] K. Eisenschmidt, T. Lanio, A. Simoncsits, A. Jeltsch, V. Pingoud, W. Wende, A. Pingoud, *Nucleic Acids Res.* **2005**, *33*, 7039.
[5] M. Pitié, C. Boldron, G. Pratviel in *Advances in Inorganic Chemistry Including Bioinorganic Studies, Vol. 58*, **2006**, pp. 77.
[6] C. Liu, M. Wang, T. Zhang, H. Sun, *Coord. Chem. Rev.* **2004**, *248*, 147.
[7] A. Sreedhara, J. A. Cowan, *J. Biol. Inorg. Chem.* **2001**, *6*, 337.

  

[8] M. Sam, J. H. Hwang, G. Chanfreau, M. M. Abu-Omar, *Inorg. Chem.* **2004**, *43*, 8447.
[9] G. Roelfes, M. E. Branum, L. Wang, L. Que, B. L. Feringa, *J. Am. Chem. Soc.* **2000**, *122*, 11517.
[10] S. Borah, M. S. Melvin, N. Lindquist, R. A. Manderville, *J. Am. Chem. Soc.* **1998**, *120*, 4557.
[11] K. Selmeczi, M. Giorgi, G. Speier, E. Farkas, M. Reglier, *Eur. J. Inorg. Chem.* **2006**, 1022.
[12] N. H. Williams, B. Takasaki, M. Wall, J. Chin, *Acc. Chem. Res.* **1999**, *32*, 485.
[13] R. T. Kovacic, J. T. Welch, S. J. Franklin, *J. Am. Chem. Soc.* **2003**, *125*, 6656.
[14] G. Q. Shangguan, J. Zhu, N. Wang, J. Z. Ni, *Chin. Chem. Lett.* **2006**, *17*, 89.
[15] R. A. Moss, K. Bracken, J. Zhang, *Chem. Commun.* **1997**, 563.
[16] W. N. Lipscomb, N. Strater, *Chem. Rev.* **1996**, *96*, 2375.
[17] G. Q. Sun, R. J. A. Budde, *Biochemistry* **1999**, *38*, 5659.
[18] F. Mancin, P. Scrimin, P. Tecilla, U. Tonellato, *Chem. Commun.* **2005**, 2540.
[19] E. Boseggia, M. Gatos, L. Lucatello, F. Mancin, S. Moro, M. Palumbo, C. Sissi, P. Tecilla, U. Tonellato, G. Zagotto, *J. Am. Chem. Soc.* **2004**, *126*, 4543.
[20] M. Nagaoka, M. Hagihara, J. Kuwahara, Y. Sugiura, *J. Am. Chem. Soc.* **1994**, *116*, 4085.
[21] P. R. Reddy, S. K. Mohan, K. S. Rao, *Chem. Biodiversity* **2005**, *2*, 672.
[22] Q. X. Xiang, J. Zhang, P. Y. Liu, C. Q. Xia, Z. Y. Zhou, R. G. Xie, X. Q. Yu, *J. Inorg. Biochem.* **2005**, *99*, 1661.
[23] L. D. Pachon, A. Golobic, B. Kozlevcar, P. Gamez, H. Kooijman, A. L. Spek, J. Reedijk, *Inorg. Chim. Acta* **2004**, *357*, 3697.
[24] P. U. Maheswari, S. Roy, H. den Dulk, S. Barends, G. van Wezel, B. Kozlevcar, P. Gamez, J. Reedijk, *J. Am. Chem. Soc.* **2006**, *128*, 710.
[25] P. de Hoog, L. D. Pachon, P. Gamez, M. Lutz, A. L. Spek, J. Reedijk, *Dalton Trans.* **2004**, 2614.
[26] G. Parkin, *Chem. Commun.* **2000**, 1971.
[27] H. Vahrenkamp, *Acc. Chem. Res.* **1999**, *32*, 589.
[28] Y. L. Wong, D. K. P. Ng, H. K. Lee, *Inorg. Chem.* **2002**, *41*, 5276.
[29] J. Reglinski, S. Morris, D. E. Stevenson, *Polyhedron* **2002**, *21*, 2167.
[30] M. Harvey, S. Baggio, R. Baggio, A. W. Mombru, *Acta Crystallogr. Sect. C* **1999**, *55*, 308.
[31] J. S. Matalobos, A. M. Garcia-Deibe, M. Fondo, D. Navarro, M. R. Bermejo, *Inorg. Chem. Commun.* **2004**, *7*, 311.
[32] A. W. Addison, T. N. Rao, J. Reedijk, J. van Rijn, G. C. Verschoor, *J. Chem. Soc. Dalton Trans.* **1984**, 1349.
[33] J. Pons, R. March, J. Rius, J. Ros, *Inorg. Chim. Acta* **2004**, *357*, 3789.
[34] A. Trosch, H. Vahrenkamp, *Z. Anorg. Allg. Chem.* **2004**, *630*, 2031.
[35] H. Y. Zhang, K. Q. Ye, J. Y. Zhang, Y. Liu, Y. Wang, *Inorg. Chem.* **2006**, *45*, 1745.
[36] A. J. Atkins, D. Black, R. L. Finn, A. Marin-Becerra, A. J. Blake, L. Ruiz-Ramirez, W. S. Li, M. Schroder, *Dalton Trans.* **2003**, 1730.
[37] S. R. Korupoju, N. Mangayarkarasi, P. S. Zacharias, J. Mizuthani, H. Nishihara, *Inorg. Chem.* **2002**, *41*, 4099.
[38] A. Sreedhara, D. Freed, J. A. Cowan, *J. Am. Chem. Soc.* **2000**, *122*, 8814.
[39] W. K. Pogozelski, T. D. Tullius, *Chem. Rev.* **1998**, *98*, 1089.
[40] A. Sokolowski, J. Muller, T. Weyhermuller, R. Schnepf, P. Hildebrandt, K. Hildenbrand, E. Bothe, K. Wieghardt, *J. Am. Chem. Soc.* **1997**, *119*, 8889.
[41] P. Chaudhuri, M. Hess, J. Muller, K. Hildenbrand, E. Bill, T. Weyhermuller, K. Wieghardt, *J. Am. Chem. Soc.* **1999**, *121*, 9599.
[42] R. C. Pratt, T. D. P. Stack, *J. Am. Chem. Soc.* **2003**, *125*, 8716.
[43] R. C. Pratt, T. D. P. Stack, *Inorg. Chem.* **2005**, *44*, 2367.
[44] P. U. Maheswari, J. Reedijk, unpublished results.
[45] E. Lamour, S. Routier, J. L. Bernier, J. P. Catteau, C. Bailly, H. Vezin, *J. Am. Chem. Soc.* **1999**, *121*, 1862.
[46] L. Benisvy, E. Bill, A. J. Blake, D. Collison, E. S. Davies, C. D. Garner, G. McArdle, E. J. L. McInnes, J. McMaster, S. H. K. Ross, C. Wilson, *Dalton Trans.* **2006**, 258.
[47] L. Benisvy, A. J. Blake, D. Collison, E. S. Davies, C. D. Garner, E. J. L. McInnes, J. McMaster, G. Whittaker, C. Wilson, *Chem. Commun.* **2001**, 1824.
[48] R. S. Nicholson, I. Shain, *Anal. Chem.* **1964**, *36*, 706.
[49] C. Boldron, P. Gamez, D. M. Tooke, A. L. Spek, J. Reedijk, *Angew. Chem.* **2005**, *117*, 3651; *Angew. Chem. Int. Ed.* **2005**, *44*, 3585.
[50] G. M. Sheldrick, SHELXS-97, University of Göttingen, Göttingen (Germany), **1997**.
[51] A. Altomare, M. C. Burla, M. Camalli, G. L. Cascarano, C. Giacovazzo, A. Guagliardi, A. G. G. Moliterni, G. Polidori, R. Spagna, *J. Appl. Crystallogr.* **1999**, *32*, 115.
[52] P. T. Beurskens, G. Admiraal, G. Beurskens, W. P. Bosman, S. Garcia-Granda, R. O. Gould, J. M. M. Smits, C. Smykalla, The DIRDIF99 program system, Technical Report of the Crystallography Laboratory, University of Nijmegen, Nijmegen (The Netherlands), **1999**.
[53] G. M. Sheldrick, SHELXL-97, Program for the refinement of crystal structures, University of Göttingen, Göttingen (Germany), **1997**.
[54] A. L. Spek, *J. Appl. Crystallogr.* **2003**, *36*, 7.
[55] R. J. Cernik, W. Clegg, C. R. A. Catlow, G. Bushnell-Wye, J. V. Flaherty, G. N. Greaves, I. Burrows, D. J. Taylor, S. J. Teat, M. Hamichi, *J. Synchrotron Radiat.* **1997**, *4*, 279.

Received: October 26, 2006
Published online: March 27, 2007

  